Title
THE EFFECT OF SPIN-ORBIT SPLITTING ON THE VALENCE BAND DENSITY OF STATES OF LEAD

Authors
McFeely, F.R.
Ley, L.
Kowalczyk, S.P.
et al.

Publication Date
1975-03-01

Submitted to Solid State Communications

LBL-3489
Preprint c.1

THE EFFECT OF SPIN-ORBIT SPLITTING ON THE VALENCE BAND DENSITY OF STATES OF LEAD

F. R. McFeely, L. Ley, S. P. Kowalczyk, and
D. A. Shirley

March 1975

Prepared for the U. S. Energy Research and
Development Administration under Contract W-7405-ENG-48

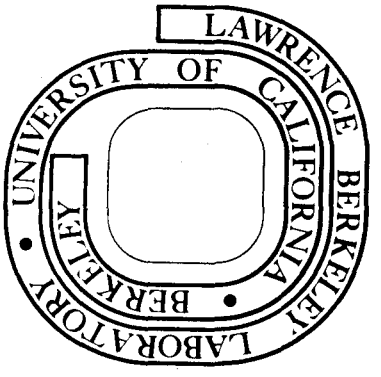

LBL-3489
c.1

DISCLAIMER

The Effect of Spin-Orbit Splitting on the Valence Band Density of States of Lead

F. R. McFeely, L. Ley, S. P. Kowalczyk and D. A. Shirley

Department of Chemistry
Lawrence Berkeley Laboratory
University of California
Berkeley, California 94720

ABSTRACT

Tight-binding calculations are reported for the valence bands of lead, with and without spin-orbit splitting in the 6p bands. The addition of spin-orbit interaction is necessary to reproduce the two-peaked structure in the 6p density of states observed in x-ray photoemission, in contrast to the assertion by Breeze that crystal-field effects alone are enough. The observed splitting is, however, only fortuitously nearly equal to the atomic spin-orbit splitting. The tight-binding band structure, with spin-orbit splitting, gives better overall agreement with optical, Fermi surface, and photoemission data than did any of the three earlier band structures.

I. Introduction

The electronic structure of metallic lead has been the subject of numerous experimental studies, mostly concerned with the elucidation of the Fermi surface. Naturally, the ultimate aim of these experiments is to provide the information necessary to construct a band structure which will explain the Fermi surface, optical spectra, photoemission spectra, and other electronic properties. Unfortunately, the difficulties involved in the calculation of a full relativistic band structure have apparently served to deter extensive first-principles calculations of the lead band structure and density of states. In an earlier paper, Ley et al.[1] reported a high-resolution x-ray photoemission (XPS) spectrum of the lead valence bands, and tentatively interpreted the two-peak structure at the top of the valence band as the result of spin-orbit splitting of the p bands. Recently, however, Breeze[2] has asserted, on the basis of a non-relativistic LCAO calculation, that the XPS splitting is instead simply the result of a crystal-field interaction. In this paper we shall re-examine the origins of this feature of the XPS spectrum by means of parametrized LCAO calculations systematically including and excluding spin-orbit coupling. We shall show that the inclusion of spin-orbit effects is essential to a consistent understanding of the XPS, optical, and Fermi surface measurements.

II. The XPS Spectrum

Figure 1 shows the XPS spectrum obtained by Ley et al.[1] using a Hewlett-Packard 5950A electron spectrometer which employed monochromatized AlK_α radiation (1486.6 eV). The high excitation energy and its concomitant featureless density of final-states insures that the

photoemission spectrum reflects the density of occupied valence band - states, modulated by cross-section and final-state relaxation effects.[3] The photoemission cross-sections of the 6s and 6p atomic states of which the valence bands are composed should be essentially equal at this energy, and outer-shell relaxation effects are small.[4] Thus the features in the valence-band spectrum should be directly proportional to the density of states N(E).

We note again the important features in the spectrum; s-like and p-like bands split by ~ 2.5 eV, a splitting of 1.8 eV in the p-like bands, and a total occupied p-bandwidth of ~ 3.5 eV.

III. The Tight-Binding Calculations

The theory of tight-binding calculations, both as first-principles calculations[5] and as the basis of interpolation schemes,[6] has been discussed extensively. Basically it consists of using tight-binding Bloch functions of the form:

$$\phi_K^n(r) = N^{-\frac{1}{2}} \sum_{\ell} e^{iK\cdot\ell}\, U^n(r-\ell) \,, \qquad (1)$$

where $U^n(r-\ell)$ is an atomic function centered at site ℓ. There is, however, a problem connected with this approach. The $\phi_k^n(r)$ are not orthogonal, because the atomic functions $U^n(r-\ell)$ centered on different sites are non-orthogonal. This entails mathematical difficulties which can be avoided by orthogonalizing the $U^n(r-\ell)$ using a procedure due to Löwdin[7] which preserves the symmetry of the atomic function. Since we do not allow for non-orthogonality of basis functions in our Hamiltonian matrix, we tacitly assume that this has been done. As Slater and Koster[5] have pointed out, however, the orthogonalization, by mixing functions on different

sites, serves to increase the distance beyond which the matrix elements connecting different sites are negligible.

In these calculations a basis of one s- and three p-functions (p_x,p_y,p_z) for each spin were used. All nearest-neighbor interactions were included, and two second-nearest-neighbor interactions of the form s-s and p-p were treated. Mixing between s and p basis functions was treated only in nearest neighbors. The largest second-nearest-neighbor integral in the final parametrization was a factor of 6 smaller than the smallest nearest-neighbor term; thus the inclusion of third-nearest-neighbor interactions would have only a negligible effect. The neglect of 3-center terms was undoubtably of greater importance.

Since Breeze[2] calculated a density of states which matched the observed spectrum width reasonably well, we began by setting the spin-orbit coupling constant equal to zero and attempting to reproduce Breeze's band structure. We were able to match Breeze's energies exactly at the points Γ, X, W, and L in the Brillouin zone. At the point K, however, while we could fit the lowest p band and the s band quite easily, the splitting $K_4 - K_1$ in the upper two p-bands was 1.8 eV in our band structure as opposed to the value of $\sim$ 2.1 eV obtained by Breeze. The band structure thus obtained and the density of states calculated at 308 points in the irreducible 1/48th of the Brillouin zone are shown in Figs. 2 and 3. We shall hereafter refer to this calculation as the "zero spin-orbit splitting" case.

In dealing with the spin-orbit splitting, it is clear from the magnitude of the atomic spin-orbit coupling constant (ξ = 0.905 eV)[8] that

this term is too large to be treated by perturbation theory. Therefore the term $\xi_{6p}(r)\ \vec{\ell}\cdot\vec{s}$ was inserted into the Hamiltonian and the resulting matrix rediagonalized. We chose to use the atomic value for the spin-orbit coupling constant since this value must be at least approximately correct for the metal; $\frac{1}{r}\frac{\partial u}{\partial r}$ is dominated by the form of the atomic potential and cannot change drastically. While agreement with experimental data could be improved by adjusting $\xi(r)$, we feel that this is physically unwarranted, since beyond a certain point "better agreement" would merely reflect the improved cancellation with errors, such as the lack of 3-center terms, inherent in our approach. The band structure and density of states from this calculation are shown in Figs. 4 and 5. The only adjustment made to facilitate the agreement with experimental results was a ~10% increase in the s-p off-diagonal matrix element.

IV. Comparisons with Experiment

In this section we shall compare the two aforementioned band structures, the 4-OPW scheme of Anderson and Gold,[9] and the relativistic APW (RAPW) calculation of Loucks[10] with the available experimental data. We shall consider the XPS, Fermi surface, and optical results in succession.

The band structures of Loucks[10] and of Anderson and Gold[9] are both in serious disagreement with the XPS results. Their primary error is that they predict values of 4.5 eV and 4.0 eV respectively for the occupied p-bandwidth. This is somewhat in excess of the experimental value of ~3.5 eV. Since both tight-binding calculations indicate that N(E) drops sharply to zero at the bottom of the p-bands, this experimental value should be quite

reliable. The OPW calculation has the further problem of giving almost no gap between the s- and p-bands while the experimental value is 2.5 eV. This splitting is, however, well matched by the RAPW calculation. Little more can be said about these band structures without actual N(E) calculations. The major conclusions are that they are somewhat too wide, and that the OPW calculation yields an anomalously small s-p band gap.

As can be seen from Figs. 2 and 3, the primary difference between the N(E) curves with and without spin-orbit splitting is the introduction of a square-shaped peak roughly 1 eV wide, centered around E_F. The origin of this peak becomes readily apparent upon comparison of the two respective band structures. In the zero spin-orbit case, there is a band crossing at 1.4 eV below E_F at the point W in the Brillouin zone. Since the slopes of the two bands near this point (W_3) are smoothly varying and non-zero everywhere in the vicinity of the crossing, there is no "peaking" of N(E) in this region. The highest energy W-point, W_2', is nearly degenerate (within ~ 0.07 eV) with X_5', and the band connecting these two points is very flat; thus N(E) "peaks" in this region, giving rise to the sharp edge of the high-energy peak in N(E), as shown in the figure.

When the spin-orbit term is introduced into the Hamiltonian, the character of the bands in the region between X and W changes. The two-fold degenerate level X_5' is split into $X_6^-(X_5')$ and $X_6^+(X_1)$, separated by 0.75 eV, and the band crossing at W_3 is lifted with the introduction of a 1.1 eV gap between the two lowest p-bands at this point. It is this lifting of degeneracies that is responsible for the changes in N(E) near the Fermi level. The primary change in this region is the appearance of a square-shaped peak from -0.2 to -1.2 eV. This peak arises almost totally

from the middle p-band between X and W. The upper (0.2 eV) edge of this peak is due to the high-state-density region near $X_6^+(X_1)$, while the lower edge arises from the $W_6(W_3)$ region. In addition to this, the opening of the 1.1 eV gap between $W_6(W_3)$ and $W_7(W_3)$ has important consequences. As can be seen in comparing the N(E) curves with and without spin-orbit splitting, N(E) has a much lower minimum at -1.5 eV with spin-orbit splitting than without. The "missing" state density shifts to lower energy, raising the -3 eV peak in N(E) and giving it a square top.

The effects of these changes on the photoemission spectra were examined by truncating the N(E) curves at E_F and broadening them with a 0.6 eV FWHM Gaussian function in order to account for instrumental resolution. The results are seen in Fig. 6. It is evident that when instrumental resolution is considered the zero-spin-orbit N(E) gives only a peak and a shoulder, while the spin-orbit split N(E) yields two peaks.

In order to test our assignment of the p-band splitting in the photoemission spectrum, we systematically varied the parameters responsible for the p-band shape. This involved bascially 3 parameters, a p-p diagonal matrix element (e.g. $\langle p_y | H | p_x \rangle$) a p-p off-diagonal matrix element, (e.g. $\langle p_x | H | p_z \rangle$), and a matrix element mixing s- and p-functions, all between nearest neighbors. There was also a second nearest neighbor p-p diagonal matrix element in the calculations; however, it was a factor of seven smaller than the smallest of the above and had a negligible affect on N(E). The observed spectrum allowed for surprisingly little variation in these parameters. The off-diagonal term determines the position of the lowest L-point and thus the total

bandwidth. Its value is therefore fixed very accurately by the experiment. In addition the lowest X point must lie very near the absolute bottom of the bands, since, if it did not, an inflection point on the high-binding-energy wing of N(E) would be apparent, where in fact none is observed. This serves as a bound on the p-p diagonal matrix element, as it largely determines the position of this X point. The s-p mixing parameter is not essentially fixed by bandwidth considerations, and thus may be varied within reasonable limits without producing glaring inconsistencies. The most important effect of the variation of this parameter is that it alters the intensity of the two peaks in the spin-orbit split simulated spectrum. It had relatively little effect on the zero-spin-orbit spectrum, never producing anything more than a peak and shoulder structure. Our final choice for the value of this parameter represented a compromise between agreement with the photoemission spectrum and with the Fermi surface data discussed below.

Anderson and Gold[9] have given a very complete discussion of their de Haas-van Alphen effect measurements for lead. The band structure they calculate matches the extremal areas of the Fermi surface very well. It is therefore likely that this band structure is reasonably accurate in predicting the values taken by the wavevector $\vec{K}$ of the bands as they cross E_F. We have calculated some of these dimensions from our spin-orbit split band structure. These are shown in Table I compared with the analogous dimensions calculated by Anderson and Gold,[9] Loucks,[10] and Breeze.[2] As can be seen, our calculations are quite comparable to the RAPW results. The one dimension, 3-11, where the discrepancy is serious

is a region in which the band is nearly flat in crossing E_F, so that any slight adjustment of E_F could improve this value greatly without significantly affecting the other dimensions.

The optical properties of Pb have also been measured by Liljenvall et al.[11] by an ellipsometric technique. Table II indicates the position of several features in the spectrum with their tentative assignments. Our calculation and the RAPW calculation would appear to yield similar results. A Kramers-Kronig extrapolation of these data, however, implies the existence of a peak at ~4.8 eV, which the authors suggest could be due to $X_6^-(X'_4) - X_6^+(X_1)$ transitions, on the basis of the RAPW band structure. If the band scheme proposed here is correct, these transitions would have to originate near the L-point. Higher energy optical data might help clarify this point. Mathewson et al.[12] generated an optical spectrum from Anderson and Gold's 4-OPW band structure[9] considering transitions throughout the Brillouin zone. As could be expected the results bore only qualitative similarity to the experimental spectrum.

Conclusions

This analysis of the Pb photoemission spectrum has shown the following:

1) The 2-peak structure in the spectrum is the direct result of spin-orbit splitting, through the lifting of degeneracies and introduction of gaps between bands and not due to the crystal field interaction, 2) The relative heights of the two peaks strongly reflects the degree of s-p mixing in the bands, 3) The observed splitting of 1.8 eV does not reflect any fundamental band splitting, but rather the placement of the Fermi level.

REFERENCES

1. LEY, L. POLLAK, R. A., KOWALCZYK, S.P. and SHIRLEY, D.A., *Phys. Letters 41A*, 429 (1972).

2. BREEZE, A., *Solid State Comm. 14*, 395 (1974).

3. FREEOUF, J. ERDUBAK, M., and EASTMAN, D. E., *Solid State Commun 13*, 771 (1973); LEY, L., POLLAK, R. A., McFEELY, F. R., KOWALCZYK, S. P. and SHIRLEY, D. A., *Phys. Rev. B 9*, 600 (1974).

4. SHIRLEY, D. A., *Chem. Phys. Lett. 17*, 312 1972.

5. SLATER, J. C. and KOSTER, G., *Phys. Rev. 94*, 1498 (1954).

6. EHRENREICH, Henry and HODGES, Laurent in Methods in Computational Physics, V. 8 pp. 149-92 (1968).

7. LÖWDIN, P. O., *J. Chem. Phys. 18*, 356 (1950).

8. MOORE, C. E. Atomic Energy Levels, National Bureau of Standards circular 467 (1949).

9. ANDERSON, J. R. and GOLD, A. V., *Phys. Rev. 139*, A1459 (1965).

10. LOUCKS, T. L., *Phys. Rev. Letters 14*, 1072 (1965).

11. LILJENVALL, H. G.,MATHEWSON, A. G. and MYERS, H. P., *Phil. Mag. 22*, 243 (1970).

12. MATHEWSON, A. G., MYERS, H.P. and NILSSON, P. O., *Phys. Stat. Sol. (b) 57*, K31 (1973).

TABLE I: Comparison of calculated Fermi surface dimensions. The notation follows Ref. 10. All distances are in atomic units.

	(a) (LCAO)	(b) RAPW	(c) OPW	(d) This work
3-4	.161	.158	.157	.162
5-6	.242	.259	.250	.244
7-9	.309	.338	.318	.322
8-9	.202	.184	.199	.193
10-11	.148	.146	.141	.167
12-13	.242	.239	.206	.251

(a) Ref. 2

(b) Ref. 10

(c) Ref. 9

(d) with $\xi_{6_p} = .905$ eV

Table II: Comparison of the prominent optical transitions with the various calculations. All energies are in eV.

	This Work (a)	RAPW (b)	OPW (c)	LCAO (d)	Expt (e)
W_6-W_7'	1.3	1.1	1.2	1.8	1.1
Σ_3-Σ_1	~1.5	~1.7	~1.4	~1.1	1.5
W_7-W_7'	2.4	2.4	2.7	1.8	2.3
?					3.8
?					4.8

(a) with ξ_{6_p} = .905 eV
(b) Ref. 10
(c) Ref. 9
(d) Ref. 2
(e) Ref. 11

FIGURE CAPTIONS

Fig. 1. X-ray photoemission spectrum of the Pb valence band region from Ref. 1.

Fig. 2. Band structure of Pb without spin-orbit coupling.

Fig. 3. Band structure, density of states, and simulated XPS spectrum of Pb, without spin-orbit coupling.

Fig. 4. Band structure of Pb including spin-orbit coupling.

Fig. 5. Band structure, density of states, and simulated XPS spectrum of Pb, including spin-orbit coupling.

Fig. 6. a) XPS valence band spectrum

b) calculated spectrum with spin-orbit coupling

c) calculated spectrum without spin-orbit coupling.

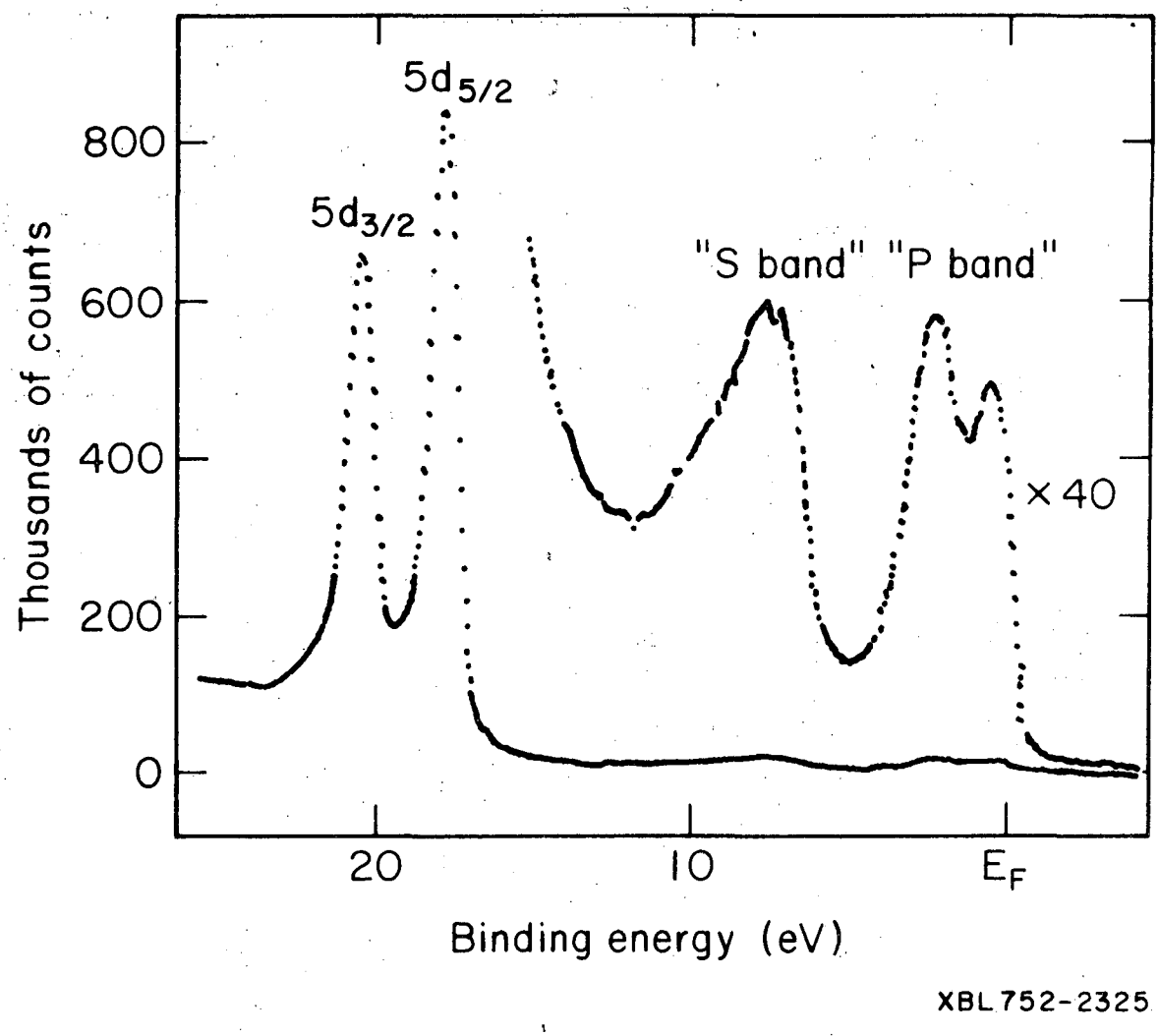

Fig. 1

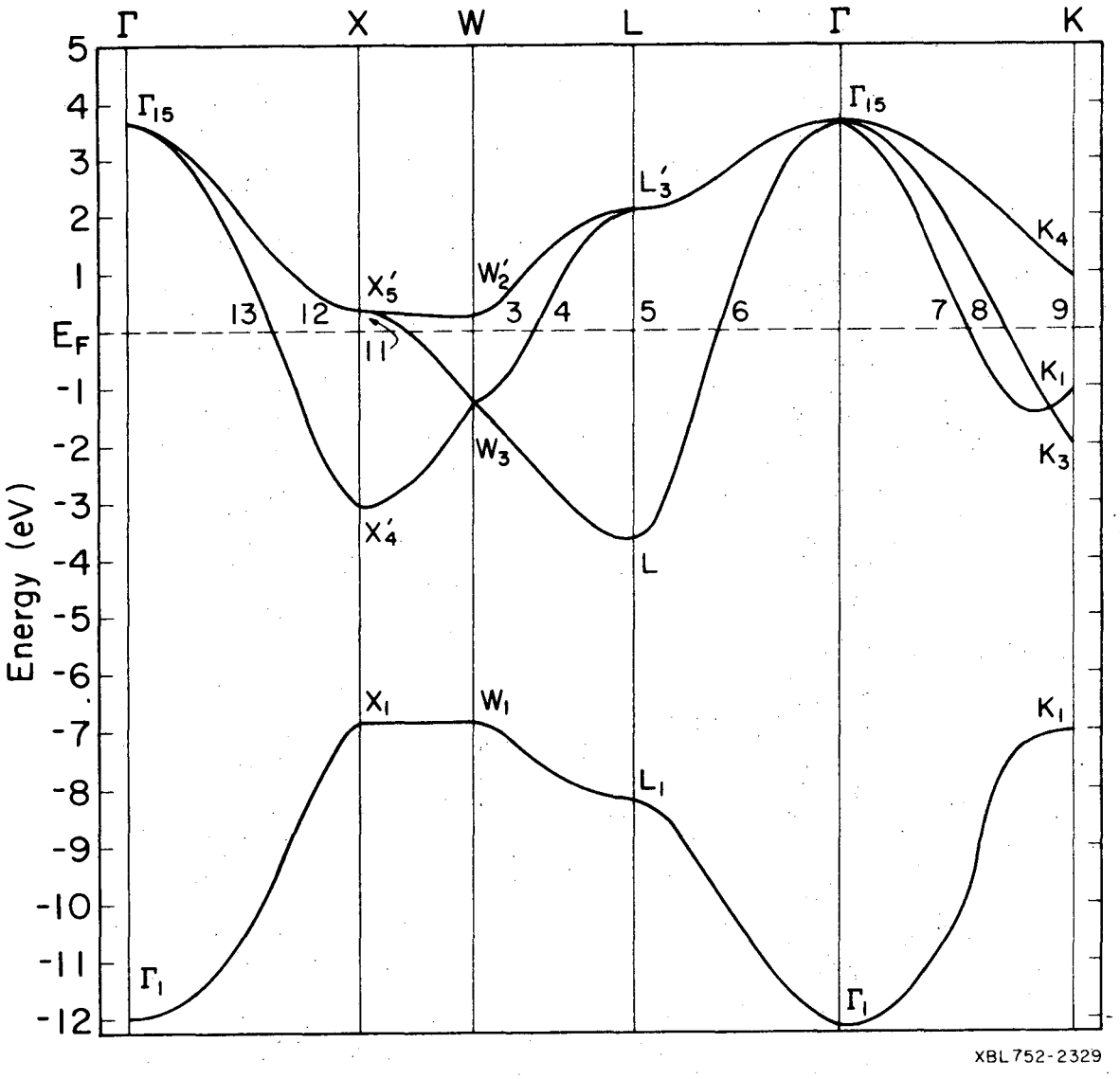
Γ
X
W
L
Γ
K
Energy (eV)
5
4
3
2
1
E_F
-1
-2
-3
-4
-5
-6
-7
-8
-9
-10
-11
-12
Γ15
X'5
W'2
L'3
K4
13
12
11
3
4
5
6
7
8
9
K1
K3
W3
X'4
L
X1
W1
L1
K1
Γ1
Γ1
XBL752-2329

Fig. 2

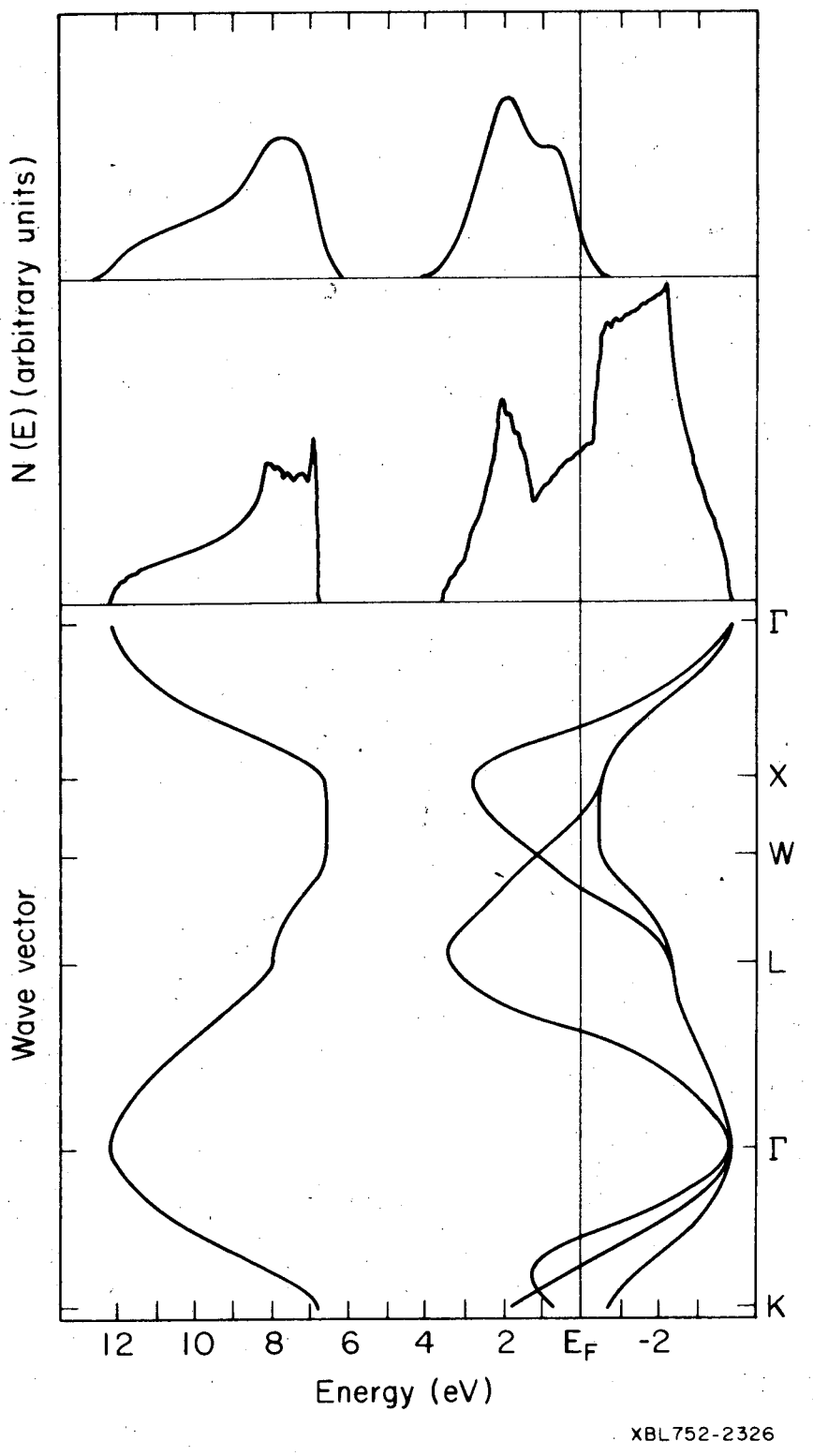
N (E) (arbitrary units)
Wave vector
Γ
X
W
L
Γ
K
12
10
8
6
4
2
E_F
-2
Energy (eV)
XBL752-2326

Fig. 3

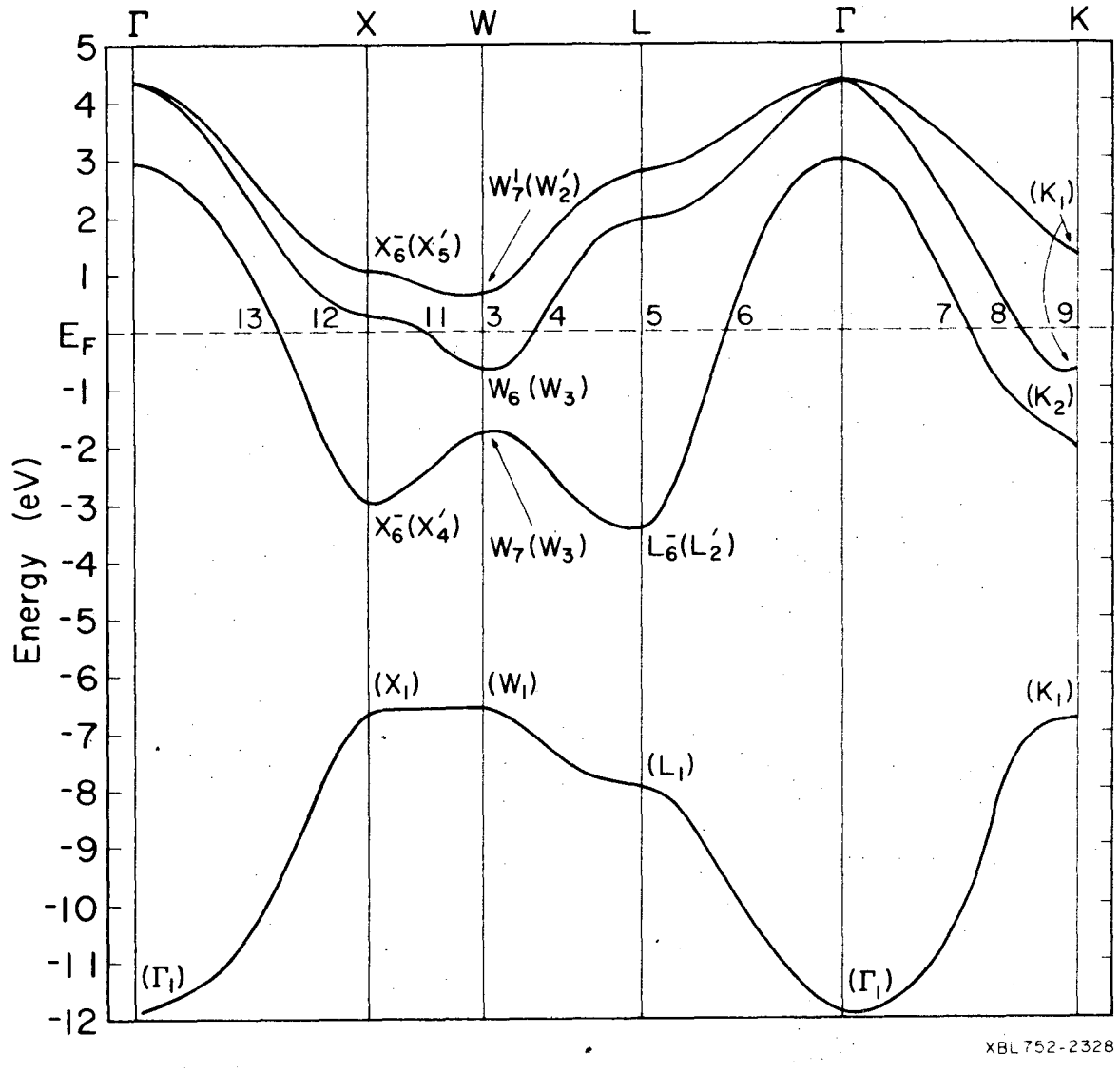
Γ
X
W
L
Γ
K
5
4
3
2
1
E_F
-1
-2
-3
-4
-5
-6
-7
-8
-9
-10
-11
-12
Energy (eV)
13
12
11
3
4
5
6
7
8
9
$W_7^1(W_2')$
$X_6^-(X_5')$
$W_6(W_3)$
$X_6^-(X_4')$
$W_7(W_3)$
$L_6^-(L_2')$
(K_1)
(K_2)
(X_1)
(W_1)
(L_1)
(K_1)
(Γ_1)
(Γ_1)
XBL752-2328

Fig. 4

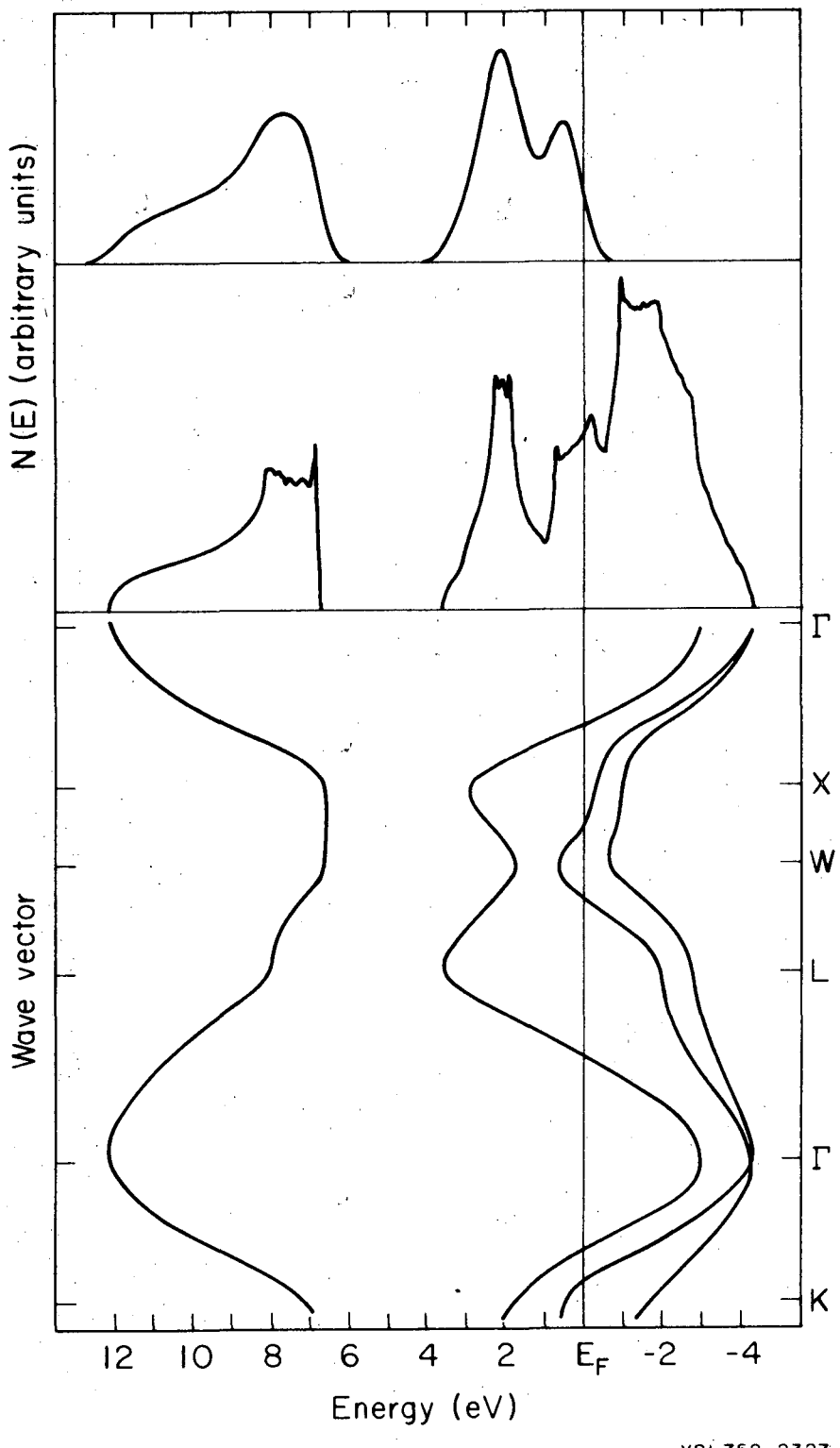
N(E) (arbitrary units)
Wave vector
Γ
X
W
L
Γ
K
12
10
8
6
4
2
E_F
-2
-4
Energy (eV)
XBL752-2327

Fig. 5

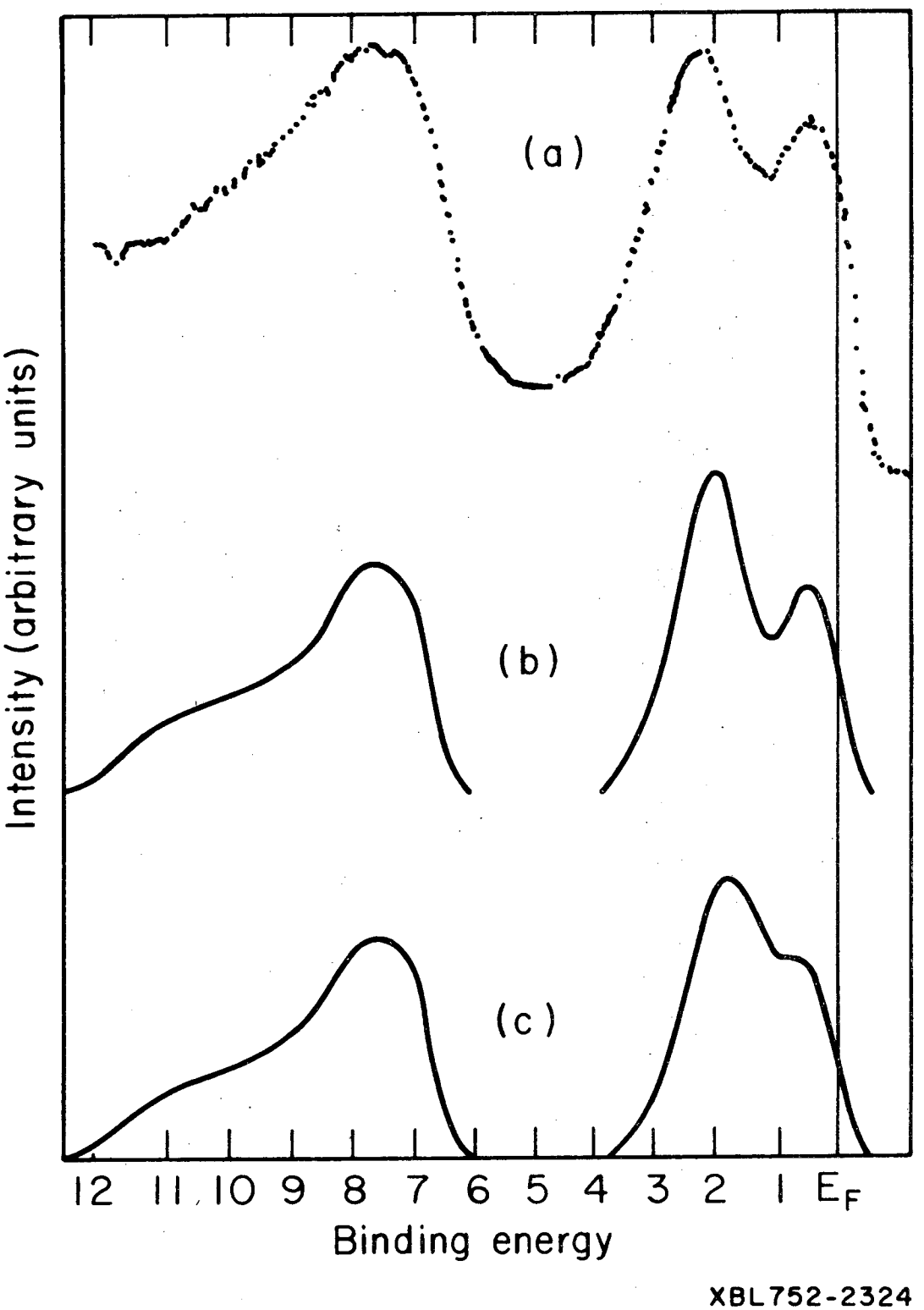
(a)
(b)
(c)
Intensity (arbitrary units)
12 11 10 9 8 7 6 5 4 3 2 1 E_F
Binding energy
XBL752-2324

Fig. 6

TECHNICAL INFORMATION DIVISION
LAWRENCE BERKELEY LABORATORY
UNIVERSITY OF CALIFORNIA
BERKELEY, CALIFORNIA 94720